Proceedings of the Korean Nuclear Society Spring Meeting
Kori, Korea, May 2000

Comparison of the PWR Cladding Corrosion models for test IFA-638.1-3

Yong-Deog Kim, Kwang-Ho Lee

Korea Electric Power Research Institute
103-16 Munji-dong, Yusung-gu
Taejeon, Korea 305-380

ABSTRACT

The cladding corrosion test (IFA-638) is being performed to investigate the corrosion properties of different modern PWR cladding materials. The experimental results are evaluated by the corrosion models, EPRI/KWU/CE, ESCORE, NEPLC, and COCHISE. The oxide layer thickness on pre-irradiated parts (upper parts) of each rod is well predicted by the COCHISE model after 118 days exposure, but the other models overpredicted the thickness. All the models overpredicted the oxide thickness after 263 days exposure and the divergency between measured and calculated oxide thickness becomes larger. The differences in calculated oxide thickness between the models at low burnup (fresh parts) are attributed to the different transition point determinations of the models. Comparing the measurements with the calculations from the pre-irradiated parts of each rod, overall overprediction could be accounted for by the fact that the post-transition regime of all these four models were calibrated for standard Zircaloy-4 materials. The differences between the models were attributed to the empirical variables such as frequency factor (k_2, B) and activation energy (Q_2) in Tables 1, 2, and 3, which were calibrated with other experimental/plant data.

1. Introduction

The cladding corrosion test (IFA-638) is performed to investigate the corrosion properties of different modern PWR cladding materials at increasing burnup/nuetron fluence levels. There are two parts to the experiment, one using fuelled cladding sections and the other using unfuelled

coupons. The materials being studied as fuelled sections are low tin Zr-2, Zr-4, high tin Zr-4, ZIRLO, M4, M5, Alloy A and E635. A total of 263 full power days (FPD) were reached for IFA-638 from the start-up in June 1998 until the end of September 1999. The 2 interim inspections were carried to measure the oxide thickness of the claddings using the eddy current technique after 125 and 263 FPD respectively. The measured oxide growth data have been evaluated by four different corrosion models, EPRI/KWU/CE[1], ESCORE[2], NEPLC[3], and COCHISE[4].

This note presents calculations and comparisons carried out with the four PWR cladding corrosion models for IFA-638.

2. Model description

2.1 Thermal Hydraulic model

All the corrosion models describe the hydraulic and thermal properties of the primary coolant under steady state or transient operating conditions.

The single channel model (SCM)[5] which has flow and enthalpy (mixing) rise factor[6] is selected in this study.

The development of a unidimensional model is based on the heat balance equation for a single, closed channel. Figure 1 gives an example of the geometrical representation used for SCM. The fuel rod of interest is rod k. Rod k is surrounded by four-coolant subchannels i and each coolant subchannel is in contact with several rods j as well as rod k.

The increase of enthalpy and the rod surface temperature (T_w) were determined from equations given by :

$$H(z,T_c(z) = FMIX\int_0^z \frac{4q''_w(z')}{GD_e}dz' \qquad (1)$$

Where,

H = enthalpy

FMIX = mixing factor

$T_C(z)$ = coolant temperature at axial location z

q''_w = rod surface heat flux

G = coolant mass flow rate

D_e = hydraulic diameter

$$T_W(z) = T_C(z) + \frac{q''_w}{h(z)[h_g(z)/h_{g\infty}]} \quad (2)$$

Where,

$T_W(z)$ = rod surface temperature at location z

h(z) = convective heat transfer coefficient at location z

$h_g(z)/h_{g\infty}$ = factor to take in account the effect of grids in promoting turbulence

In two-phase flow heat transfer conditions, the rod surface temperature is expressed as a function of saturation temperature (T_{sat}) and rod surface super heat(T_{sat})[7] :

$$T_w(z) = T_{sat} + \Delta T_{sat} \quad (3)$$

Where, T_{sat} is given by Thom' s correlation[8] :

$$\Delta T_{sat} = 72 \times \{(q''_w / 10^6\}^{0.5} \times \exp(-P_{ref}/1260) \quad (4)$$

ΔT_{sat} = $T_w(z)$ - T_{sat} (^oF)

T_{sat} = saturation temperature (^oF)

q'' = rod surface heat flux (Btu/h-ft^2)

P_{ref} = system pressure (psi)

2.2 Corrosion model

Several PWR cladding corrosion models have been developed for interpreting Zircaloy-4 cladding oxide data and predicting oxide thickness for fuel reload design applications. With proper interpretation of high burnup oxide data, it is anticipated that cladding corrosion behavior can be more accurately predicted and better corrosion reduction strategies can be devised.

The four different corrosion models, which are published, EPRI/KWU/CE, ESCORE, NEPLC, and COCHISE are represented in Tables 1, 2, and 3. The Zircaloy corrosion process being

essentially a diffusion-controlled reaction, for all the semi-empirical models, Zircaloy oxidation kinetics are represented by Arrhenius equations by comparison with diffusion laws as a function of temperature. The main parameter determining the corrosion rate is the temperature at the interface between cladding and oxide. Accordingly the clad-to-coolant heat transfer correlation and the thermal conductivity of the oxide are important factors when modeling the corrosion of a cladding. Since different correlations and values have been used when calibrating the different corrosion models, the values of these parameters also have to be considered when comparing the different corrosion models. All of the models include a pre-transition region with a cubic corrosion rate, followed by a post-transition region where the corrosion rate is constant with time.

Table 1. Kinetic variables and correlations of EPRI/KWU/CE and ESCORE model.

Model	Equation	Variables
EPRI/KWU/CE	***Pre-transition*** $\frac{ds}{dt} = \frac{A}{s^2} \cdot \exp(\frac{-Q_1}{RT})$, ***At transition*** $s_t = D \cdot \exp(-\frac{Q_3}{RT} - E \cdot T)$, ***Post-transition*** $\frac{ds}{dt} = B \cdot \exp(\frac{-Q_2}{RT})$ $B = C + \delta \cdot U \cdot (M \cdot \varphi)^p$	s = oxide layer thickness [μm] t = time [day] T = temperature at the interface between metal and oxide [K] s_t = Transition Thickness [μm] φ = fast neutron flux (>1 MeV) [n/cm^2/s] R = 1.9858 cal/mol K Q1 = 32289 cal/mol Q2 = 27354 cal/mol Q3 = 10763 cal/mol A = 6.3e9 μm^3/day, C = 8.04e7 μm^3/day D = 2.14e7 μm, E = 1.17e-2K^{-1} M = 7.46e-15 cm^2 s/n, P = 0.24 U = 2.59e8 μm/day
ESCORE	Based on EPRI/KWU/CE Model $B = C + U \cdot (M \cdot \varphi)^p$	$M = 1.91e-15 \ \text{cm}^2 s/n$ $U = 2.38e8 \ \mu m/day$

Table 2. Kinetic variables and correlations of NEPLC model.

Model	Equation	Variables
COCHISE	***Pre-transition*** $\frac{ds}{dt} = \frac{k_1}{s^2} \cdot \exp(\frac{-Q_1}{RT})$, ***At transition*** $t_t = D_3 \cdot \exp(\frac{Q_3}{RT} - E_3 \cdot T)$, ***Post-transition*** $\frac{ds}{dt} = k_2 \cdot \exp(\frac{-Q_2}{RT})$	s = oxide layer thickness [μm] t_t = Transition time [day] T = temperature at the interface Between metal and oxide [K] R = 1.9858 cal/mol K Q1 = 34119 cal/mol Q2 = 36542 cal/mol Q3 = 1830 cal/mol K_1 = 11.4e10 μm^3/day K_2 = 4.0e11 μm E_3 = 3.5e-2 K^{-1} D_3 = 8.857e10 day

Table 3. Kinetic variables and correlations of COCHISE model.

Model	Equation	Variables
COCHISE	***Pre-transition*** $\frac{ds}{dt} = \frac{k_1}{s^2} \cdot \exp(\frac{-Q_1}{RT})$, ***At transition*** $t_t = D_3 \cdot \exp(\frac{Q_3}{RT} - E_3 \cdot T)$, ***Post-transition*** $\frac{ds}{dt} = k_2 \cdot \exp(\frac{-Q_2}{RT})$	s = oxide layer thickness [μm] t_t = Transition time [day] T = temperature at the interface Between metal and oxide [K] R = 1.9858 cal/mol K Q1 = 34119 cal/mol Q2 = 36542 cal/mol Q3 = 1830 cal/mol K_1 = 11.4e10 μm^3/day K_2 = 4.0e11 μm E_3 = 3.5e-2 K^{-1} D_3 = 8.857e10 day

3. PWR corrosion model calculations

3.1 Fuel rod geometries and operating conditions of the IFA-638

Three tests rods were installed in IFA-638. Each rods is composed of four segments prepared from a combination of fresh and pre-irradiated materials, as shown in Figure 2. Each segment

comprises aproximately 120 mm of cladding material with an O.D. of 9.5 mm and I.D. of 8.25 - 8.36 mm. The six segments of the pre-irradiated materials were mechanically defuelled, and filled with 8 wt% U-235 enriched UO_2 pellets to an active fuel stack length of 90 mm. The bottom two segments of the each rod are fresh fuel rod segments with same enriched UO_2 pellets and same active fuel stack length as the pre-irradiated segments (upper parts).

The coolant outlet and inlet temperature and the pressure in the rig were kept at about 317 ℃, 310 ℃, and 159 bar respectively, while the inlet flow rate was maintained at 1.9 and 1.2 m/s for IFA-638.1-2 and IFA-638.3 respectively. The average linear heat rate (ALHR) for the test assembly was between 22 and 32 kW/m during operation of IFA-638.1, 638.2, and 638.3.

3.2 Corrosion model input data

The following operating data are required for the time-dependent average core power history, the rod geometry and thermohydraulic characteristics of the core, which are independent of time such as :

mass flow rate of the primary coolant, coolant inlet temperature, and core pressure.

The average linear heat rate and fast neutron flux of the rods are averaged for 60 time steps and 12 axial power shapes with the time step were used to describe the power history. The active length of each rod is divided into up to 20 axial nodes. The initial local conditions at each of these nodes for each rod are input and the oxide layer thickness calculated according to the equations in Tables 1, 2, and 3. The thermal conductivity of ZrO_2 is an important factor in determining the metal-oxide interface temperature, and the default values for each model, which are used in this study, presented in Table 4.

The experimental corrosion data for comparison with the values predicted by the different models were obtained by eddy current measurements.

Table 4. The ZrO_2 thermal conductivity values used in the different models.

Model	K_{ox}(W/cm-K)
EPRI/KWU/CE	0.015
ESCORE	0.015
COCHISE	0.016
NEPLC	s < 48 ㎛ : 0.015 s < 48 ㎛ : $(3.48-0.0412*s)*10^{-2}$ s < 48 ㎛ : 0.008 ---------- s : oxide thickness

3.3 Calculated results

The oxide growth rates as a function of axial segment elevation are investigated. The measured

and calculated results obtained from the 3 rods after 118 and 263 FPD irradiation are shown in Figures 3 to 8.

Note : The measured data for segment 2(high tin Zircaloy-4) of rod 1 were not available after 263 days exposure because of oxide spalling and the measured oxide thickness data of rod 3(M4 & M5 alloys) after 118 days were not available at the time of writing this report, since the measured data were still being reviewed on the basis of new calibrations for the alloys.

3.3.1 The un-irradiated segment parts

Considering the fresh material parts (lower parts) of each rod, the oxide thickness calculations of all models underpredicted measured values by up to 50 % after 118 days exposure. The NEPLC model, however, showed good agreement for 263 days exposure, while the COCHISE and EPRI/KWU/CE - ESCORE models overpredicted (~ +50 %) and underpredicted (~ -42 %) respectively.

3.3.2 The pre-irradiated segments parts

The oxide layer thickness on pre-irradiated parts (upper parts) of each rod is well predicted by the COCHISE model after 118 days exposure, but the other models overpredicted the thickness. All the models overpredicted the oxide thickness after 263 days exposure and the divergency between measured and calculated oxide thickness becomes larger. The maximum difference (about 91 %) between measured and calculated oxide thickness increase on segment 2(alloy M5) of rod 3 was obtained with the EPRI/KWU/CE model.

4. Discussion of the comparison results

As seen from Figures 3 to 8, the EPRI/KWU/CE and ESCORE models underestimate corrosion rates for the fresh parts of each rod until 263 days exposure and the COCHISE model calculation underpredicts after 118 FPD and overpredicts after 263 FPD, while the NEPLC model shows good agreement for 263 days exposure. The differences in calculated oxide thickness between the models at low burnup are attributed to the different transition point determinations of the models. As shown in the equations in Tables 1, 2 and 3, the EPRI/KWU/CE and ESCORE models calculate transition point as an oxide thickness with the metal-oxide interface temperature and the COCHISE model calculates the transition time, whilst the NEPLC model uses a fixed value of 1.98 W/cm-K. The transition point calculation of the models with the metal/oxide interface temperature is illustrated in Figure 9 and 10. The transition time in the EPRI/KWU/CE and ESCORE models, and the transition thickness in the

COCHISE model can be calculated by the pre-transition correlations in Tables 1 and 3. The transition thicknesses and times of the EPRI/KWU/CE and ESCORE models vary from 2.05 to 2.53 ㎛ and 2865.8 to 245.6 days with variations in metal-oxide temperature from 300 to 370 ℃. The transition thicknesses and times of the COCHISE model varies from 2.11 to 2.61 ㎛ and 862.9 to 62.5 days within the same temperature range. If we assume the metal-oxide interface temperature to be 613 K, the transition time of the EPRI/KWU/CE and ESCORE models is 703.9 days, while that of the COCHISE model is 191.6 days. Thus, the transition point of the COCHISE model is reached faster than the EPRI/KWU/CE and ESCORE models.
Comparing the measurements with the calculations from the pre-irradiated parts of each rod, overall overprediction could be accounted for by the fact that the post-transition regime of all these four models were calibrated for standard Zircaloy-4 materials. The differences between the models were attributed to the empirical variables such as frequency factor (k_2, B) and activation energy (Q_2) in Tables 1, 2, and 3, which were calibrated with other experimental/plant data. As a remark, a corrosion model which has been calibrated for clad materials used in this experiment is recommended for further evaluations.

5. Summary and conclusions

The cladding corrosion test (IFA-638) is being performed to investigate the corrosion properties of different modern PWR cladding materials. The experimental results are evaluated by the corrosion models, EPRI/KWU/CE, ESCORE, NEPLC, and COCHISE.
When comparing the measured and the predicted oxide thickness, the following conclusions can be drawn ;

1. Considering the fresh material parts (lower parts) of each rod, the oxide thickness calculations of all models underpredicted measured values by up to 50 % after 118 days exposure. The NEPLC model, however, showed good agreement for 263 days exposure, while the COCHISE and EPRI/KWU/CE - ESCORE models overpredicted (~ +50 %) and underpredicted (~ -42 %) respectively.

2. The oxide layer thickness on pre-irradiated parts (upper parts) of each rod is well predicted by the COCHISE model after 118 days exposure, but the other models overpredicted the thickness. All the models overpredicted the oxide thickness after 263 days exposure and the divergency between measured and calculated oxide thickness becomes larger.

3. The differences in calculated oxide thickness between the models at low burnup (fresh parts) are attributed to the different transition point determinations of the models.

4. Comparing the measurements with the calculations from the pre-irradiated parts of each rod, overall overprediction could be accounted for by the fact that the post-transition regime of all these four models were calibrated for standard Zircaloy-4 materials. The differences between the models were attributed to the empirical variables such as frequency factor (k_2, B) and activation energy (Q_2) in Tables 1, 2, and 3, which were calibrated with other experimental/plant data.

References

1. A.M.Garde, et al., Waterside Corrosion of Zircaoy Fuel Rods, EPRI NP-2789, Research Project 1250-1, Combustion Engineering, Inc., December 1982.
2. R.B.Fancher, I.B.Fiero, H.R.Freeburn, A.M.Garde, M.W.Kennard, M.A.Krammen, P.G.Smerd and N.T.Yackle, ESCORE the EPRI Steady-State CoreReload Evaluator Code: General Description, EPRI Report, NP-5100, February 1987.
3. H.E.Evans, M.V. Polley, A Review of the NFIR-I Zircaloy Corrosion Projects, Volume 3: Code Predictions of In-Reactor Corrosion, EPRI NP-7320-D, Volume 3, Nuclear Electric PLC, September 1992.
4. Ph.Billot, A.Giordano, Comparison of Zircaloy Corrosion Models from the Evaluation of In-Reactor and Out-of-Pile Loop Performance, Zirconium in the Industry: Ninth International Symposium, ASTM STP 1132, pp.539-565, 1991.
5. K.D.Sheppard, et al., Analysis of Zircaloy Oxide Thickness Data from PWRs, EPRI NP-6698, Research Project 1250-18, S.M.Stoller Corporation, February 1990.
6. K.D.Sheppard, A.A.Strasser, Evaluation of the EPRI/GAZAROLLI Zircaloy Corrosion Model for U.S. Reactors, IAEA Technical Committee Meeting on Fundamental Aspects of Corrosion of Zircaloy Base Alloys in Water Reactor Environments, Portland, Ore., 11-15 September 1989.
7. R.H.S.Winterton, Thermal Design of Nuclear Reactors, Chapter 5, University of Birmingham, England, 1981.
8. J.R.S.Thom, W.M.Walker, T.A.Fallon, and G.F.S.Reising, Boiling in Subcooled Water During Flow in Tubes and Annuli, Proc. Inst. Mech. Engr., 3C180:226, 1965-66.

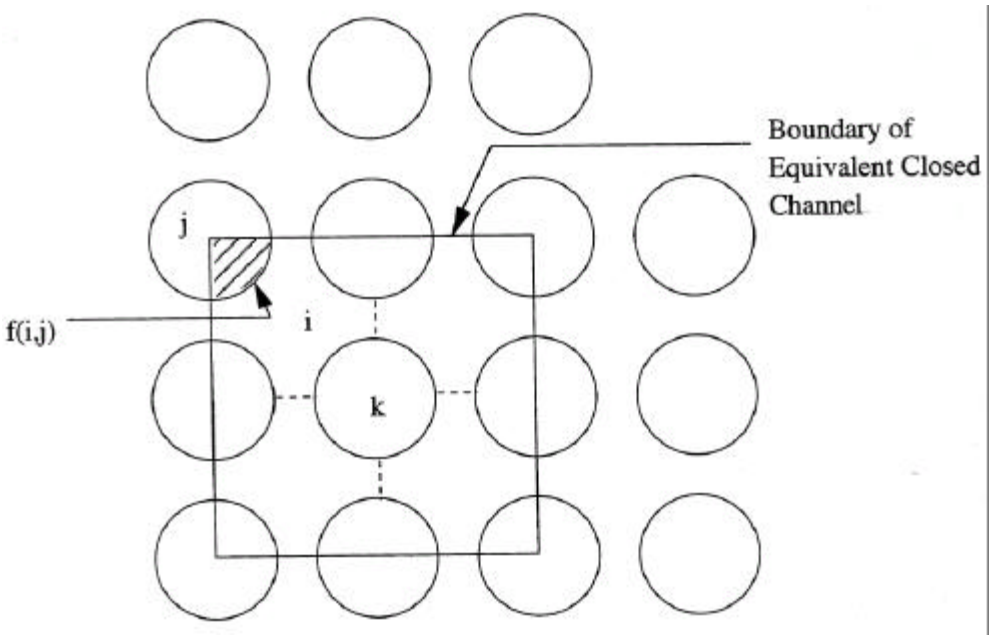

Figure 1. Geometrical description of channels for thermal hydraulic model.

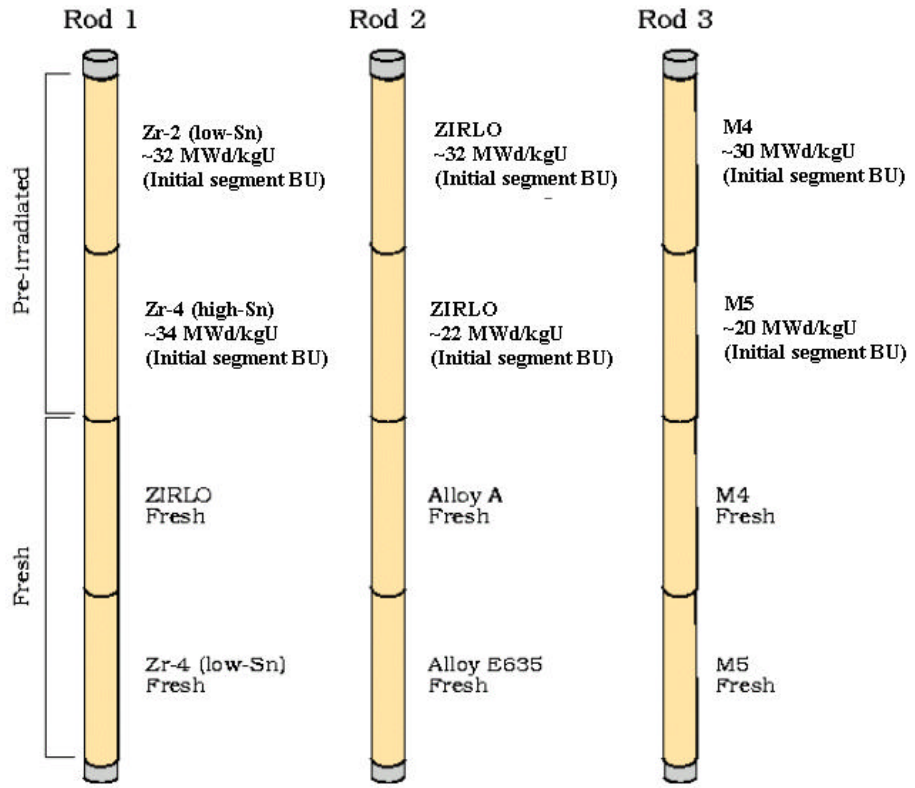

Figure 2. Schematic lay-out of the fuel rods used in the PWR cladding corrosion test, IFA-638.

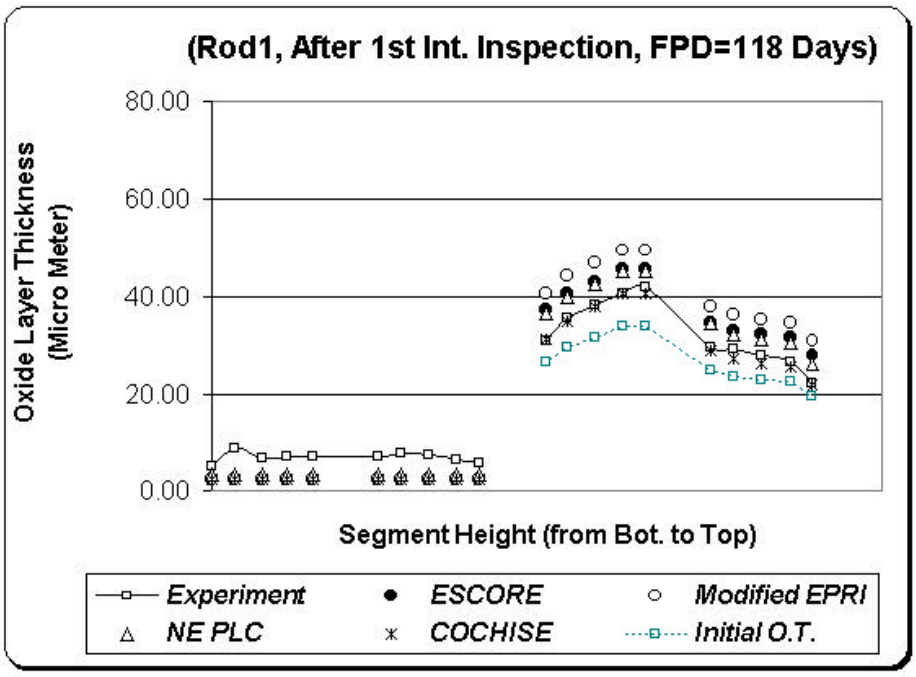

Figure 3. Comparison of measured and calculated oxide thickness for IFA-638 rod 1 after 118 FPD.

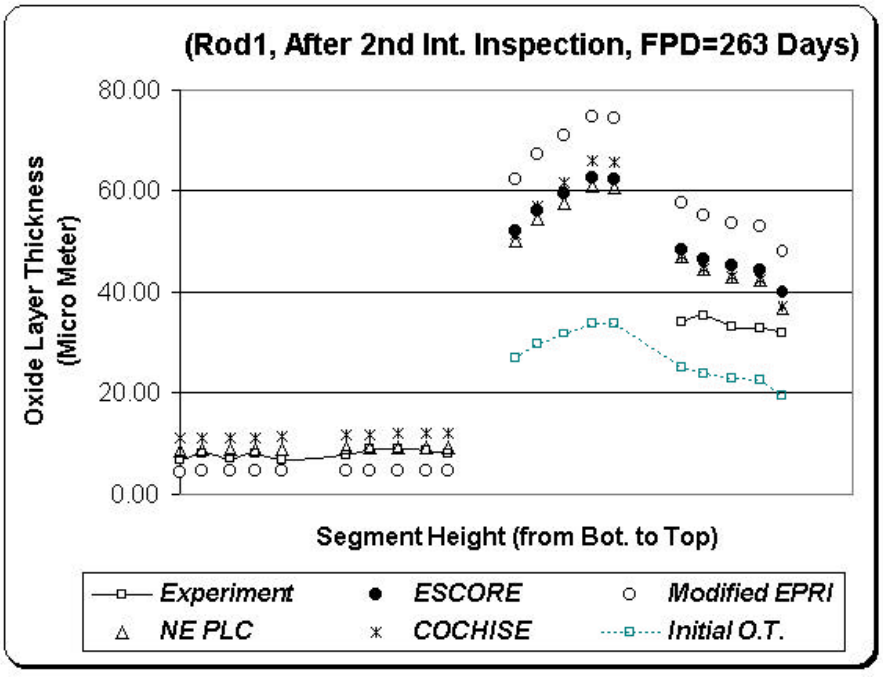

Figure 4. Comparison of measured and calculated oxide thickness for IFA-638 rod 1 after 263 FPD.

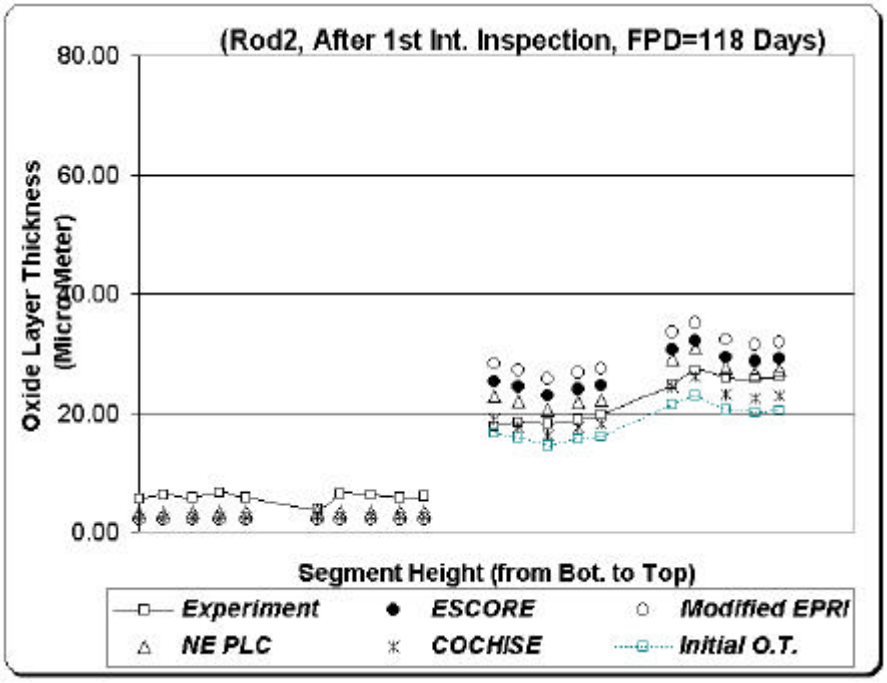

Figure 5. Comparison of measured and calculated oxide thickness for IFA-638 rod 2 after 118 FPD.

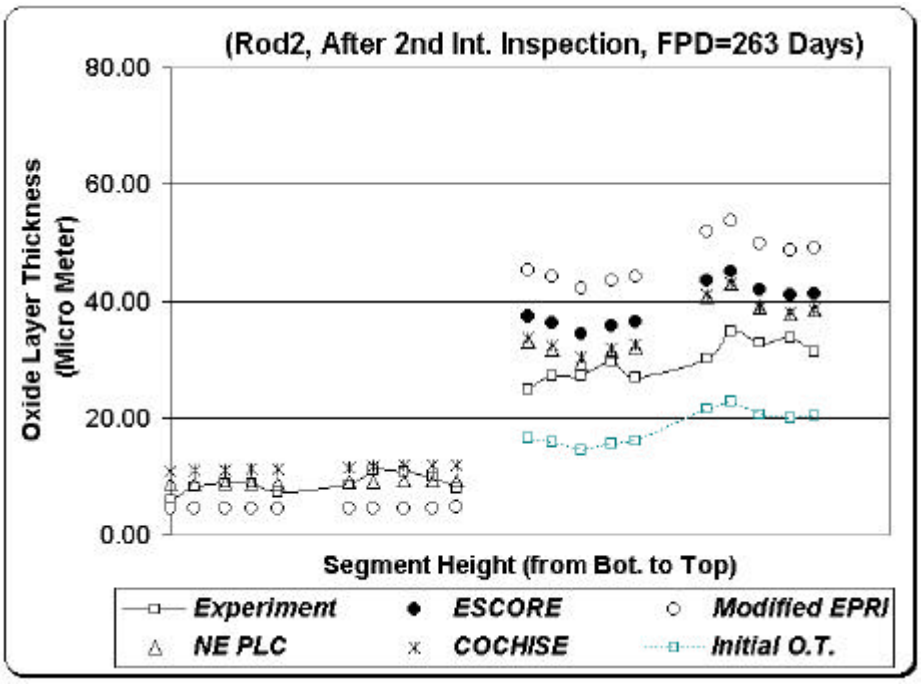

Figure 6. Comparison of measured and calculated oxide thickness for IFA-638 rod 2 after 263 FPD.

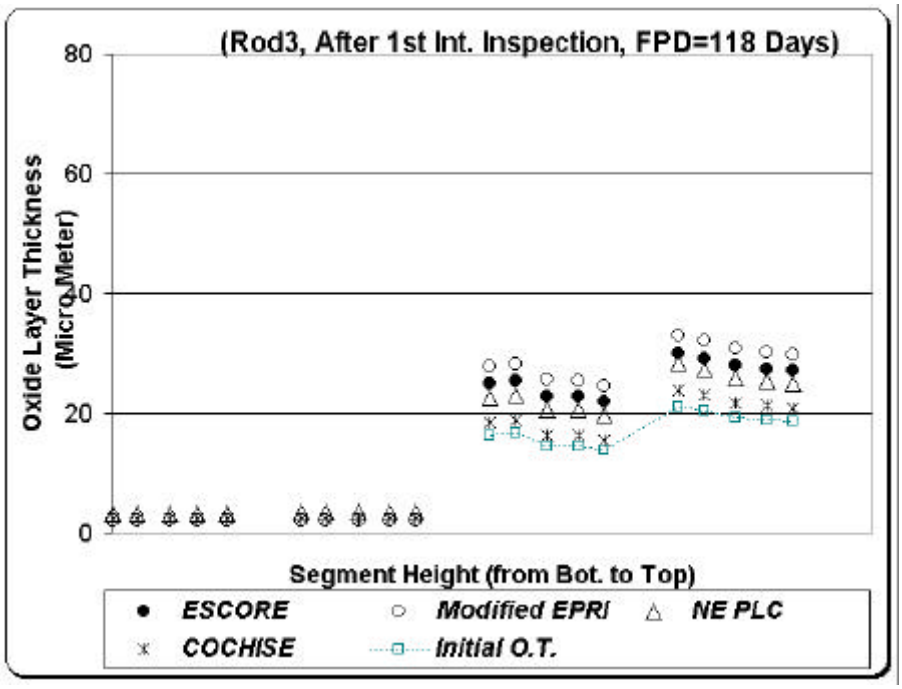

Figure 7. Comparison of measured and calculated oxide thickness for IFA-638 rod 3 after 118 FPD.

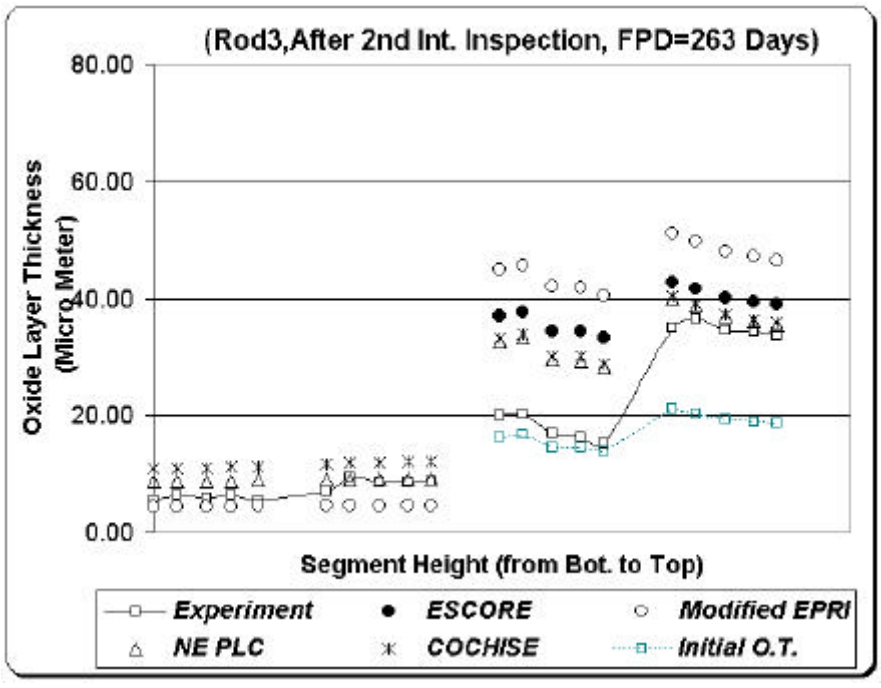

Figure 8. Comparison of measured and calculated oxide thickness for IFA-638 rod 3 after 263 FPD.

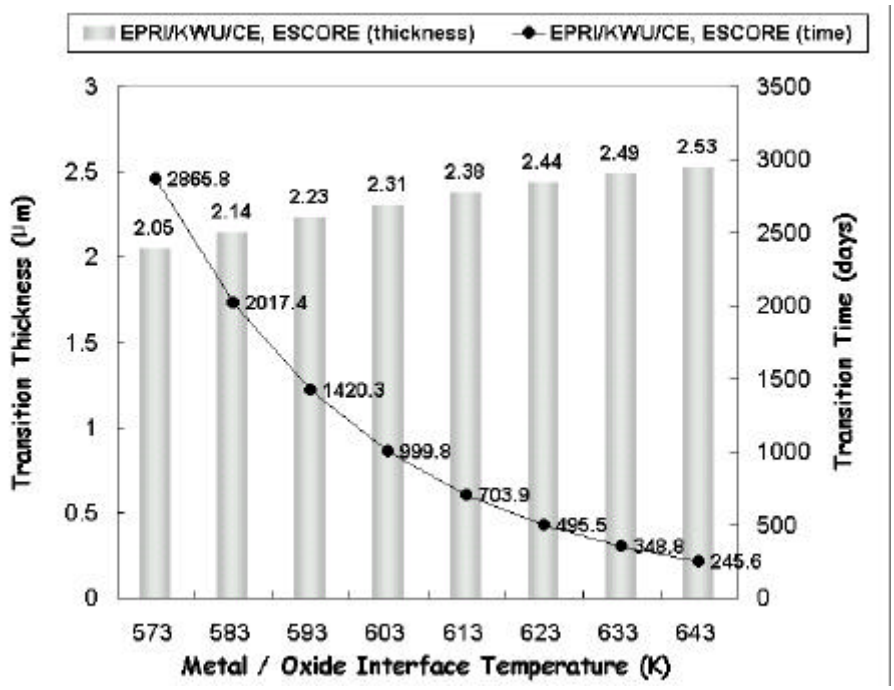

Figure 9. Transition point calculation with temperature of the EPRI/KWU/CE and ESCORE corrosion models.

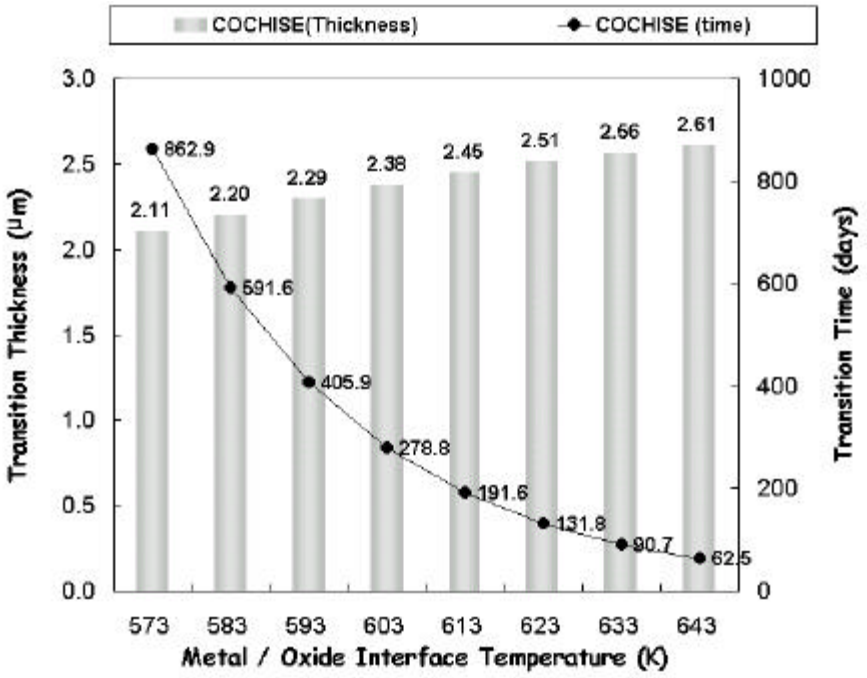

Figure 10. Transition point calculation with temperature of the COCHISE corrosion model.